1-20-2020

Evidence of Ridge Propagation in the Eastern Gulf of Mexico from Integrated Analysis of Potential Fields and Seismic Data

Irina Filina
University of Nebraska-Lincoln, ifilina2@unl.edu

Mei Liu
University of Houston, mliu30@uh.edu

Erin Beutel
College of Charleston, beutele@cofc.edu

Published in *Tectonophysics* 775 (January 20, 2020), 228307; doi: 10.1016/j.tecto.2019.228307

Submitted January 4, 2019; revised November 23, 2019; accepted December 1, 2019; published online December 14, 2019.

Evidence of Ridge Propagation in the Eastern Gulf of Mexico from Integrated Analysis of Potential Fields and Seismic Data

Irina Filina,[1] Mei Liu,[2] and Erin Beutel[3]

1. Department of Earth and Atmospheric Sciences, University of Nebraska–Lincoln, Lincoln, Nebraska, USA
2. Department of Earth and Atmospheric Sciences, University of Houston, Houston, Texas, USA
3. Department of Geology and Environmental Geoscience, College of Charleston, Charleston, South Carolina, USA

Corresponding author – Irina Filina, email ifilina2@unl.edu

Abstract

Integrated analysis of gravity, magnetic, and seismic data reveals two phases of spreading in the eastern Gulf of Mexico (GOM) including two distinct spreading centers, suggesting a major ridge reorganization during the opening of the eastern part of the GOM. Ridge propagation between the two spreading episodes explains the following observations: (1) the drastic asymmetry in the oceanic domain of northeastern GOM, (2) the presence of two distinct crustal zones with dramatically different thickness and physical properties, and (3) the observed seismicity within the oceanic domain that is not aligned with any known tectonic structure. The initial Late Jurassic spreading center (~160 Ma) resulted in a thin (~5 km) and uniform oceanic crust with a fast compressional velocity (7 km/s). Based on our analysis, the estimated full spreading rate of this older spreading event is less than 1 cm/yr. The spreading regime changed in Early Cretaceous around 150 Ma, resulting in a propagation (i.e., jump) of the spreading center. The new spreading episode was characterized by a change in spreading direction and increased magma supply as it produced thicker (up to 9 km) oceanic crust with a typical two-layered structure. Despite the increase in magmatic material, the full rate of this younger spreading event estimated from our analysis is only slightly faster (1.1 cm/yr assuming that

spreading ceased at 137 Ma). The later conclusion is consistent with the morphology of the spreading centers mapped by seismic data. Our analysis shows that recent deep crustal earthquakes in the middle of the Gulf of Mexico are aligned with the boundary between the two identified distinct oceanic zones, referred to here as a pseudofault.

1. Introduction and motivation for the study

The Gulf of Mexico (GOM) is an oceanic basin in the southeastern part of North America that opened during the breakup of the Pangaea starting in Triassic (Galloway, 2009). The details of the basin's formation are still being debated, although the overall consensus implies continental rifting started in Triassic, followed by the oceanic spreading in Jurassic, which eventually ceased in Early Cretaceous (Pindell and Kennan, 2009; Kneller and Johnson, 2011; Hudec et al., 2013; Eddy et al., 2014; Christeson et al., 2014; Nguyen and Mann, 2016; Pindell et al., 2016; Lundin and Doré, 2017). The formation of oceanic crust was associated with the rotation of the Yucatan crustal block counterclockwise from North America; however, the location of the Ocean-Continent Boundary (OCB) and the pre-breakup location of this block as well as the total rotation angle vary in different models (see Fig. 1, also Bird et al., 2005; Kim et al., 2011, Lundin and Doré, 2017).

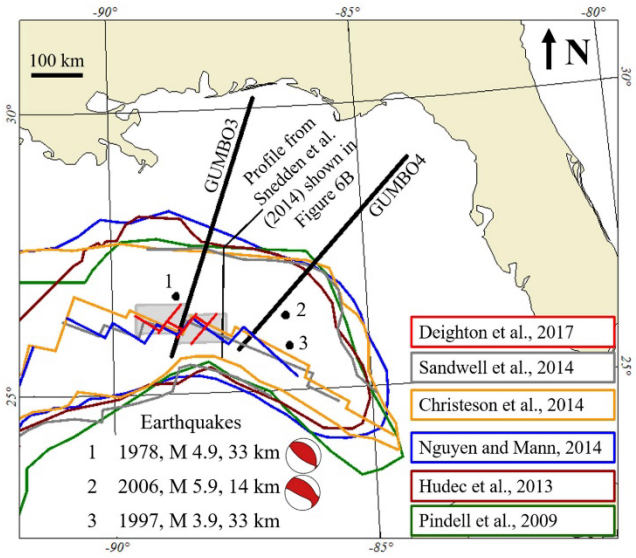

Figure 1. The study area is in the eastern Gulf of Mexico. Two thick black lines represent the GUMBO3 and GUMBO4 profiles from Eddy et al. (2014) and Christeson et al. (2014); the thin black line shows the location of seismic reflection profile from Snedden et al. (2014) shown in Fig. 6B. The gray box outlines the 3D seismic reflection survey from Deighton et al. (2017). The Ocean-Continent boundaries (OCB) and the segments of the extinct spreading centers with the associated transform faults from different published models are shown by different colors. Three black dots show the locations of deep earthquakes (from the USGS catalog); only two of these have published focal mechanisms, suggesting the overall compressional stress oriented NE-SW.

We have made several observations that are challenging to explain with the current tectonic models. Our first observation is the striking asymmetry of the Gulf of Mexico ocean floor about the currently mapped spreading center (Fig. 1). The location of a spreading center was mapped by several authors from the satellite gravity data (Sandwell et al., 2014; Nguyen and Mann, 2016), from magnetic data (Pindell et al., 2016) and from 2D and 3D seismic surveys (Eddy et al., 2014; Christeson et al., 2014; Snedden et al., 2014; Deighton et al., 2017). Some authors have noticed the striking asymmetry in the volume of oceanic crust of the eastern GOM (Hudec et al., 2013; Nguyen and Mann, 2016), which is difficult to explain with symmetrical spreading. Seismic refraction profiles GUMBO3 and GUMBO4 imaged approximately 165 km and 145 km of oceanic crust respectively between the OCB in the north and the extinct spreading centers (Eddy et al., 2014; Christeson et al., 2014; Fig. 2). Christeson et al. (2014) report a full-spreading rate of 2.2 cm/yr for GUMBO 4, assuming that the spreading started at 152–155 Ma and ceased at 138–142 Ma. The estimates for GUMBO3 are slightly higher (2.4 cm/yr, Eddy et al., 2014). However, these estimates apply only to the oceanic crust to the north of the identified spreading center (Fig. 1); the oceanic zone to the south of the spreading center is dramatically narrower (between 80 and 100 km) and would yield a much slower spreading rate. Up to date, it is not clear how these two presumably conjugate oceanic segments of drastically different widths were produced over the same time period, assuming, as the literature does, a single spreading episode for the eastern Gulf of Mexico.

Second, there are remarkable differences in the oceanic crustal structure within the Gulf of Mexico, specifically, two distinct oceanic crustal zones with drastically different thickness and physical properties. The GUMBO3 refraction experiment runs from coastal Alabama SSW toward the center of the Gulf of Mexico (Eddy et al., 2014; Fig. 2A) and images thick (up to 9 km) oceanic crust with a somewhat typical two-layered structure—a 2- to 3-km-thick top layer with the compressional seismic velocity Vp from 5.5 to 6 km/s, presumably composed of basalts, which overlies a thicker layer with Vp of 7 km/s, presumably gabbroic (Fig. 2A). However, the accompanying seismic reflection experiment (Eddy et al., 2014; Fig. 2B) refined the crustal structure as up to 3 km thinner near the OCB, while maintaining the thick (~9 km) crust toward the center of the basin. The more eastern refraction line, which runs from Florida SW into the Gulf of Mexico, GUMBO4 (Fig. 2C), suggests strikingly different oceanic structure—much thinner (~5 km) oceanic crust with uniform Vp values of 7 km/s, presumably composed of gabbro. The apparent lack of basaltic layer along GUMBO4, as well as dramatic thinning of the produced crust, suggest different spreading regime with respect to GUMBO3. Thus, it appears that two spreading regimes existed in the northeastern Gulf of Mexico, one that produced thin, gabbroic oceanic crust (predominantly close to the OCB) and one that produced layered thick oceanic crust closer to the middle of the basin.

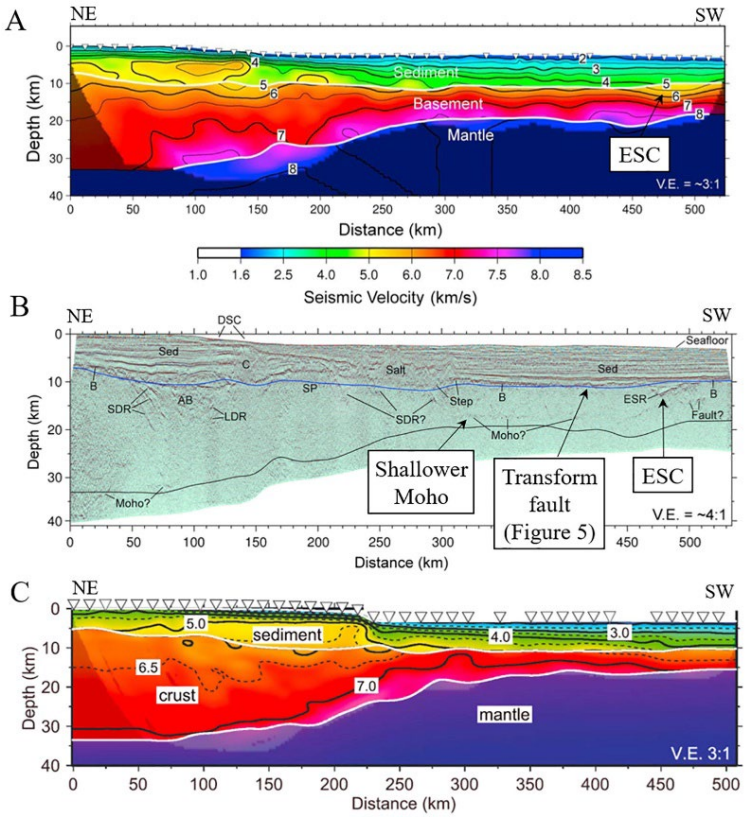

Figure 2. Seismic cross-sections through the study area. (A) Refraction profile GUMBO 3 (Eddy et al., 2014); the Extinct Spreading Center (ESC) at the SW end of the line is associated with a noticeable drop in seismic velocities. (B) Seismic reflection profile (coincident with GUMBO3) from Eddy et al. (2014). The extinct spreading center (ESC), denoted as ESR (extinct spreading ridge) by Eddy et al. (2014), is marked by a pronounced trough in basement. Blue and black lines show the depths from refraction to basement and Moho respectively. Note the strong reflectivity in the oceanic domain suggesting the shallower Moho; AB—Apalachicola Basin, B—basement from seismic reflection, C—carbonate platform, DSC—De Soto Canyon, LDR—landward dipping reflector; SDR—seaward dipping reflector; SP—Southern Platform. (C) Seismic refraction line GUMBO4 (Christeson et al., 2014). Note strikingly different structure of oceanic crust with respect to GUMBO3—much thinner and uniform crust with faster seismic velocities. (For interpretation of the references to color in this figure legend, the reader is referred to the web version of this article.)

A third observation that is not accounted for by any published tectonic models is the presence of three recorded earthquakes in the eastern Gulf of Mexico (Fig. 1) with focal depths of 14 km and 33 km, suggesting their lithospheric nature. Two of these (1 and 2 in Fig. 1) are located far away from the interpreted extinct spreading center, and it is not clear what tectonic structure they are aligned with. Focal mechanisms are available for these two earthquakes published by the USGS (https://earthquake.usgs.gov) and are strikingly similar (Fig. 1), suggesting the release of compressional stress along NW-SE striking fault. Although

this orientation is generally aligned with the ridge segments identified in the GOM, the epicenters are ~60 km to the north of the identified ridges.

In this study, we have utilized an integrative approach to geophysical data analysis (Filina, 2019). We have performed spatial analysis of gravity data, constrained with available seismic reflections and refractions data and validated with magnetic data to map major tectonic structures in the eastern GOM in order to explain the three observations listed earlier: (1) the striking asymmetry of the oceanic domain, (2) the remarkable differences in the oceanic crustal structures between GUMBO3 and GUMBO4, and (3) the presence of deep crustal seismicity away from known tectonic structures. Our analysis resulted in new constraints for the tectonic reconstruction of the Gulf of Mexico. Based on our joint interpretation of gravity, magnetic, and seismic data, we suggest that the basin experienced a major ridge reorganization during the opening, offering a novel way to reconstruct the eastern Gulf of Mexico.

2. Material and methods

The gravity field from Sandwell et al. (2014; Fig. 3A) and magnetic data from Lubinski and Twichell (1989; Fig. 3B) were utilized to study the crustal organization in the eastern GOM. The observed potential fields represent cumulative signals from the rocks with different physical properties in the subsurface, namely with different densities and magnetic susceptibilities. Subsurface layers include water (nonmagnetic, density of 1.03 g/cm^3,Telford et al., 1990), very low-magnetic sediments with densities varying from 2 to 2.6 g/cm^3, crustal units with densities and magnetic susceptibilities depending on the nature (oceanic crust is generally denser and more magnetic than continental) and on the location within the crust (the upper crust is less dense and less magnetic than the lower one), and finally the nonmagnetic upper mantle with density in order of 3.3 g/cm^3. The general principle of potential fields states that anomalies are generated by lateral variations in physical properties, not by vertical ones. In other words, if all subsurface layers were flat (i.e., layer cake model), there would be flat gravity and magnetic responses without any anomalies observed. In contrast, the lateral variations in physical properties, such as changing thicknesses of individual layers and/or contacts between various types of rocks (such as Ocean-Continen boundary) will result in potential fields anomalies.

In this study, we are particularly interested in the signals from the oceanic crustal structures. In order to highlight them, we applied a number of processing steps to remove signals that interfere with or impact the crustal signal. In gravity, we have removed the effects of water and the Moho (i.e., the topmost and the deeper subsurface layers). The gravity effect of the water overlying the sedimentary section (i.e., Bouguer correction, Telford et al., 1990) was computed using the bathymetry data from Smith and Sandwell (1997) with assumed sediment density of 2 g/cm^3. The gravity signal of the deepest source—the effect of the crust-mantle interface (i.e., Moho), often referred to as a regional trend, was not directly computed as the depth to Moho in not well constrained for the study area. In contrast, it was derived via mathematical procedure of upward continuation (Telford et al., 1990) of the Bouguer gravity anomaly. This procedure extrapolates the observation plane of gravity field to the higher level, resulting in a dampening of the shallow-source (i.e., high

frequency) gravity anomalies and leaving behind only broad and low-frequency signals from the deep sources (i.e., regional trend). In this study, we used an elevation of 30 km to generate a regional trend. This value was chosen by trial and error as the one sufficiently removing the high-frequency gravity signatures.

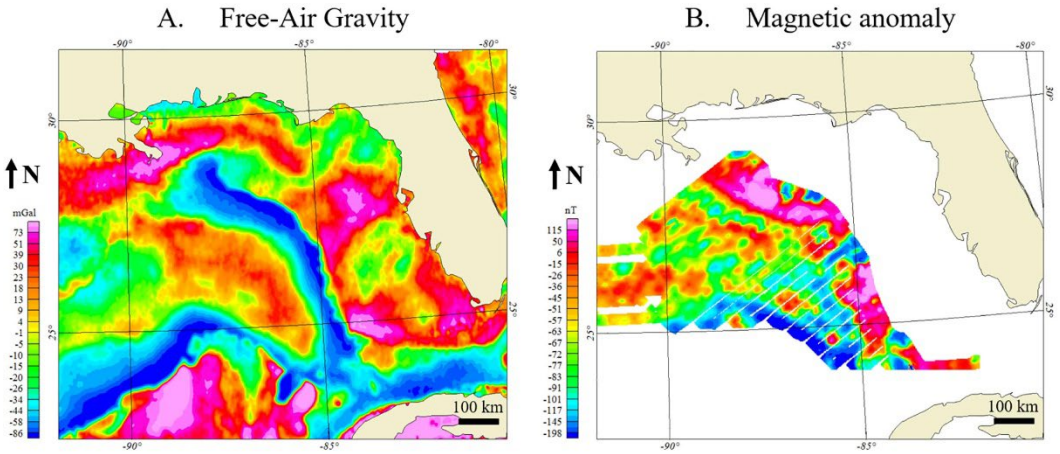

Figure 3. Potential fields data used for the study. (A) Free-Air Gravity field from Sandwell et al. (2014). This dataset was used for spatial analysis and mapping major tectonic structures. (B) Marine magnetic data from Lubinski and Twichell (1989). The quality of this dataset did not allow for comprehensive spatial analysis. This dataset was used for validation of the derived results (see magnetic profile in Fig. 6C).

The regional trend was removed from the Bouguer gravity anomaly, resulting in the residual gravity field that includes the signatures of the sedimentary layers and crustal structures. Since the focus of our study is in the oceanic domain that is away from salt structures, the sedimentary section comprises a series of semi-flat layers without notable lateral variations (as seen in seismic sections), so it does not produce noteworthy and highly variable gravity anomalies. Therefore, most of the observed signals in the residual gravity anomaly are related to structures within the crust that are associated with significant contrasts in the rock densities. These structures result in lineated patterns of gravity anomalies called lineaments. The most pronounced lineaments are associated with the boundary between continental and oceanic domains (i.e., OCB) that represents a significant contrast in density as oceanic rocks are generally denser than continental ones. Similarly, integrated geophysical modeling determined the rocks of the extinct spreading center are less dense with respect to the adjacent oceanic crust (Liu and Filina, 2018). This decrease in crustal density over the extinct spreading center correlates well with the observed drop in seismic velocities Vp recorded in both GUMBO3 and GUMBO4 (Fig. 2A, C). The apparent drop in Vp corresponds to a decrease in density, leading to negative anomalies in gravity over the extinct spreading centers. The series of mathematical transformations (i.e., filters) were applied to the residual Bouguer anomaly in order to choose the

one that highlights the lineaments better. We used a high-pass filter with 100 km window of the residual Bouguer gravity (Fig. 4) for further analysis.

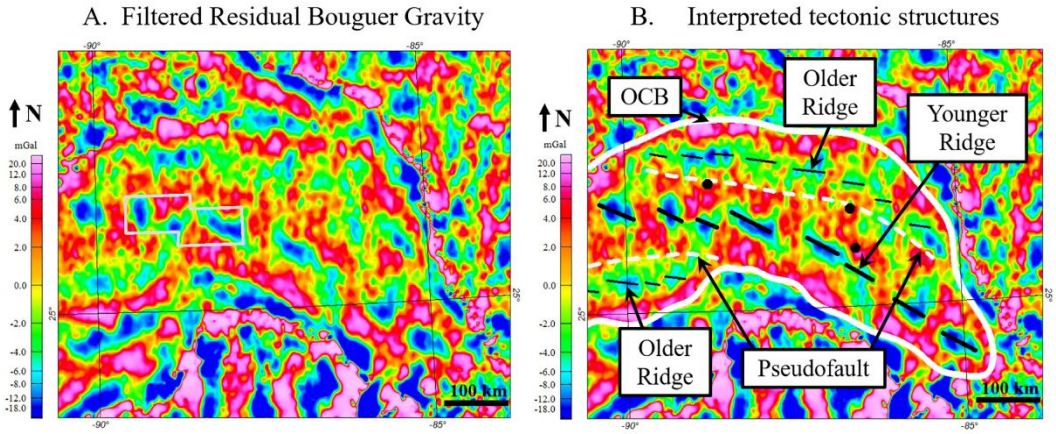

Figure 4. Filtered gravity field (uninterpreted A, with interpretation B); refer to text for filtering details. Pronounced lineaments in both fields corresponding to OCB (onset of gravity high, white line) and extinct spreading center (gravity lows) are clearly observed. Two spreading systems are identified: the younger one (thick black) in the center and the old ones in the northeast and southwest (thin black segments). The boundary between two oceanic domains produced in each phase—referred to as a pseudofault—is marked with a dashed white line. Three black dots show the location of earthquakes from Figure 1. The gray box in section A shows the extent of 3D seismic survey from Deighton et al. (2017) shown in Figure 5.

In magnetics, the effect of sediments is several orders less than the signature of much more magnetic crustal rocks, so we assume that observed magnetic anomalies relate to the contrast in magnetic susceptibilities of the crustal rocks. The recorded magnetic anomalies (Fig. 3B) are skewed due to the nonverticality of the ambient field. To correct for that, a reduction to the pole filtering was applied using the ambient field parameters computed for the magnetic epoch of 1985 (the year of the marine magnetic survey). The ambient field was computed with Geomag 7.0 software (Thébault et al., 2015). In general, the sampling interval between magnetic profiles was up to 30 km (Fig. 3B), which does not allow for performing a comprehensive spatial analysis. We also tried to apply similar filtering to a public domain magnetic data (Meyer et al., 2017), unsuccessfully, however, due to a low spatial resolution of that magnetic dataset. Therefore, only gravity data were used to map tectonic structures, while magnetic data were used to validate our interpretation.

3. Results and discussion

The spatial analysis of filtered residual gravity anomalies revealed pronounced lineaments (Fig. 4) that confirmed or enhanced previously identified features such as the Ocean-Continent

boundary (OCB) and the central extinct spreading ridge; however, it also identified new apparent extinct spreading ridges in the anomalous ocean crust.

The location of the OCB, confirmed with several seismic lines (Eddy et al., 2014; Christeson et al., 2014; Snedden et al., 2014) and with integrated modeling (Liu and Filina, 2018), is well aligned with the onset of the obvious gravity high (Fig. 4B), allowing us to trace that boundary outside of seismic coverage for the entire study area. The segments of the central extinct spreading center can be interpreted from the filtered gravity field as pronounced lows (Fig. 4, thick black lines) that correlate very well with the results of other authors (Fig. 1), as well as with seismic data (Figs. 2, 5, and 6B). Deighton et al. (2017) mapped the extinct spreading center associated with basement valleys from 3D seismic survey in the study area (Fig. 5; see the location of the 3D seismic survey in Figs. 1 and 4A). Given the confirmation of existing features, we feel confident in using the same technique to identify new structures.

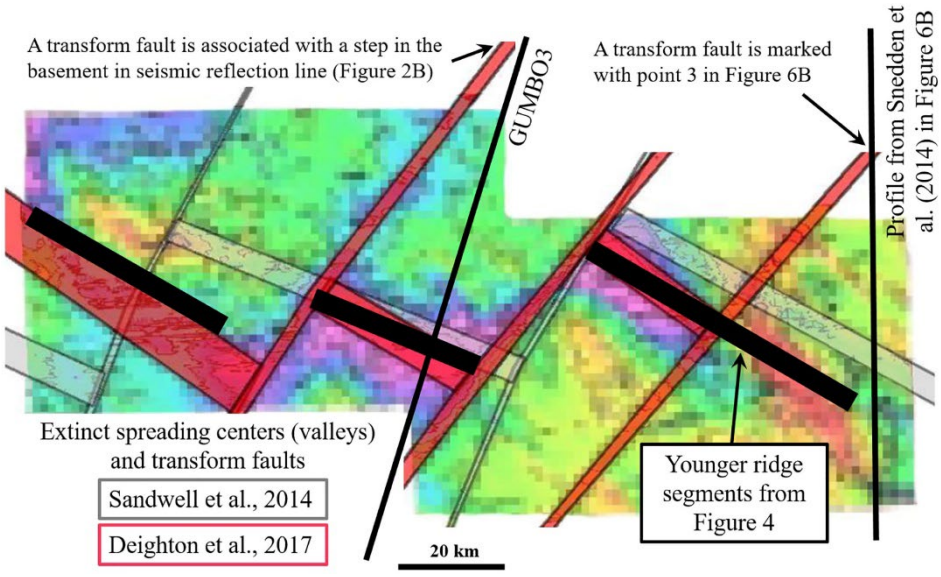

Figure 5. The interpreted spreading system (valleys associated with young ridge) from our analysis (thick black lines) over the depth to basement map derived from 3D seismic survey by Deighton et al. (2017). Note that the proprietary data from Deighton et al. (2017) are obscured in the initial publication. The series of spreading valleys (purple colors) offset by transform faults is mapped in seismic; it agrees very well with gravity lows in filtered data (marked with thick black lines). The two tectonic interpretations are superimposed by Deighton et al. (2017): the gray color shows the spreading centers and transform faults from Sandwell et al. (2014), while the red color shows the interpretation of Deighton et al. (2017). The interpreted transform faults are observed as steps in the basement in seismic reflection data (Figs. 2B and 6B).

We identified a series of smaller features in the oceanic domain to the northeast and the southwest of the interpreted intact spreading system. Their appearance in the filtered gravity field is similar to the previously identified extinct spreading center but of smaller extent.

We propose that these features are the remnants of an initial spreading episode in the eastern GOM, presumably starting at ~160 Ma (age from Snedden et al., 2014). This implies that the ridge reorganization occurred during basin opening and resulted in the jump of the spreading center (Figs. 4 and 6). The presumably older spreading system (in older crust) appears to trend more east-west while the previously identified younger spreading system is more northwest-southeast orientated (Fig. 4B). Further evidence of the presence of two spreading systems can be found in the changes in crustal thickness and structure seen in Figure 2. The change from a thin and uniform oceanic crust to a thicker and layered oceanic crust occurs between the identified older spreading center and the younger spreading center and appears to be visible in the gravity as well as in the seismic (Figs. 4 and 6B). The boundary between the two oceanic domains, referred to as pseudofault (dashed white line in Fig. 4B) marks a change in the spreading style and direction, which suggests a change in the tectonic regime and should mark a change in the Euler pole. While most reconstructions of the Gulf of Mexico use a single Euler pole, Pindell et al. (2016) proposed a Euler pole jump at 150 Ma, which may reflect this change in spreading direction and style.

The older spreading centers, oriented more E-W, are associated with the thin, homogenous, high-density oceanic crust in the GUMBO3 and GUMBO4 seismic lines (Fig. 2). Previous studies, using both seismic profiles and ophiolites, observed that thin, more uniform crust is associated with ultra-slow spreading centers as described at the Greenland-Norwegian Mohns Ridge (e.g., Chen, 1992; White et al., 1992; Bown and White, 1994; Klingelhöfer et al., 2000; White et al., 2001). Our analysis shows that the older crustal segment in the north produced thin crust that is on average 96 km wide (Fig. 4). Using the spreading initiation age of ~160 Ma from Snedden et al. (2014) and ridge reorganization at ~150 Ma from Pindell et al. (2016), we estimate the full spreading rate of the older ridge as 0.9 cm/yr (ultra-slow). Therefore, we propose that thinner and uniform crust from GUMBO4 (Fig. 2C) was produced during initial ultra-slow spreading. This is analogous to the ultra-slow spreading via detachment faulting over the Southwest Indian Ridge described by Sauter et al. (2013) that resulted in a thinner, more uniform crust. Hence, this suggests that the onset of spreading in the Gulf of Mexico was ultra-slow and associated with the E-W ridges before a change in spreading around 150 Ma (age from Pindell et al., 2016).

Ocean crust adjacent to the previously identified NW-SE trending spreading center appears to be significantly different from the crust around the E-W spreading centers; the area around the younger NW-SE spreading center is layered like typical ocean crust (Fig. 2A). Although it appears to be thicker than typical ocean crust, thicker crust has been previously observed at both slow and ultra-slow spreading centers has been associated with periods of greater magma supply (e.g., Seher et al., 2010; Jian et al., 2017). Our analysis suggests that the younger spreading system in the center of the basin produced crust that is 146 km wide on average (Figs. 4 and 6), and assuming the ridge reorganization at ~150 Ma (consistent with Pindell et al., 2016) and the spreading cessation at ~137 Ma (Snedden et al., 2014), we estimate a slightly faster spreading rate (1.1 cm/yr) for the younger ridge. The latter one is consistent with the overall morphology of the younger extinct spreading centers that are imaged in seismic data as valleys, not as ridges (Christeson et al., 2014; Eddy et al., 2014; Deighton et al., 2017; Saunders et al., 2016), supporting the overall conclusion about slow spreading rate. The two valleys associated with each of the spreading phases

can also be seen in seismic profile from Snedden et al. (2014) shown in Figure 6B. The boundary between the two oceanic crustal segments (point 2 in Fig. 6) represents the pseudofault created as the ridge reorganization occurred. The reduced to pole magnetic data (Fig. 6C) support our interpretation of two spreading centers (marked with magnetic high) divided by magnetic low associated with interpreted pseudofault.

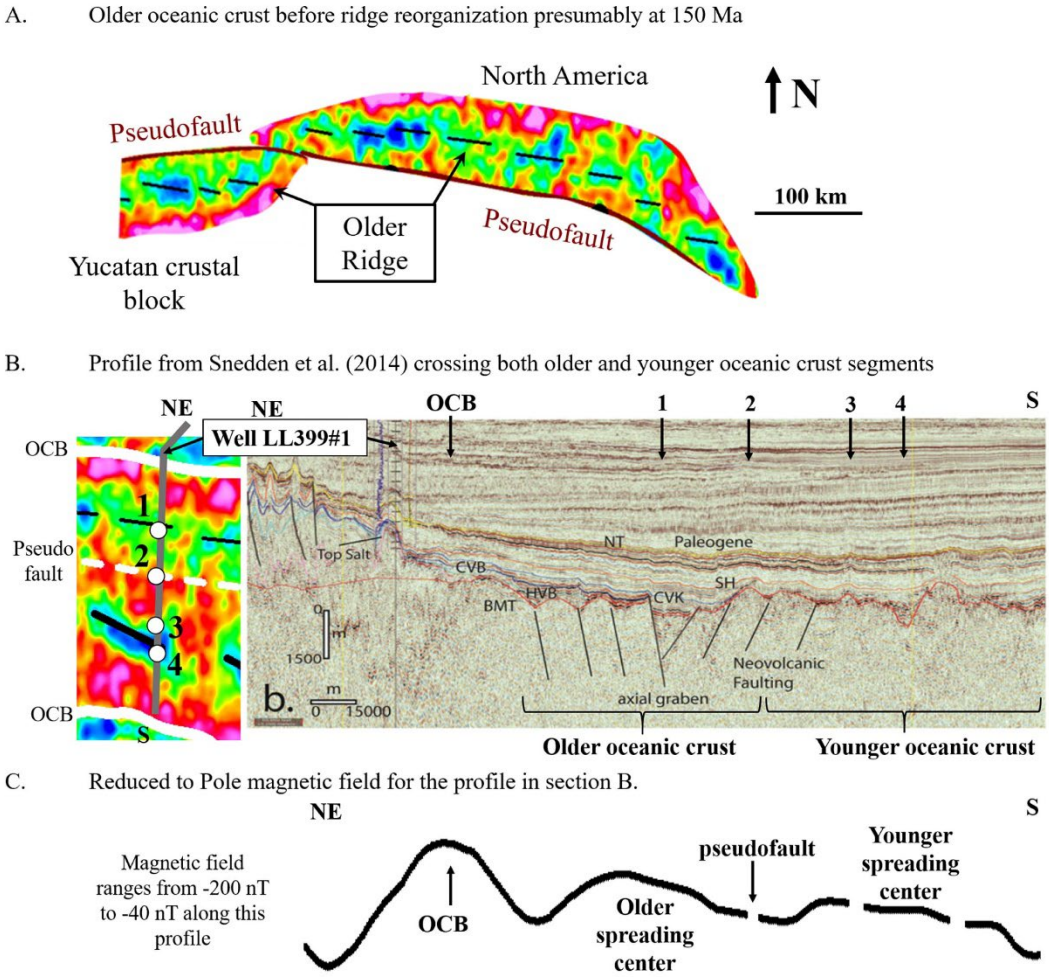

Figure 6. (A) The restoration of the older spreading system and oceanic crust before the ridge reorganization (the segments are from Fig. 4B). (B) Seismic cross-section from Snedden et al. (2014) crossing both older and younger oceanic crust segments. The inset map is a fragment of Figure 4B that illustrates the correlation of the individual structures observed in seismic data with the features in filtered gravity field. The notations in seismic section are from Snedden et al. (2014) and include basement (BMT) and the following supersequences: CVB is Cotton Valley–Bossier, HVB is Haynesville-Buckner, CVK is Cotton Valley–Knowles, SH is Sligo-Hosston, and NT is Navarro-Taylor. (C) Reduced to pole magnetic data from Figure 3B. The spreading centers correspond to magnetic highs, while interpreted pseudofault is aligned with magnetic low.

Thus, we have identified what appears to be a ridge reorganization in the Gulf of Mexico that represents both a change in the spreading direction from N-S to NE-SW and a change in magma supply. To determine the viability of the geometry we observed, we compared the interpreted geometries for the ridge reorganization in our study area with the known propagated spreading center over the East Pacific Rise (EPR) shown in Figure 7. The EPR is a much younger feature that is not covered with a thick sedimentary layer and thus is clearly seen in bathymetry data. Figure 7A shows the bathymetric expression of the ridge reorganization from the fossil ridge in the east (the Galapagos Rise) to the younger active one (EPR) in the west. The EPR is a fast-spreading ridge and cannot be considered as a proper analog for a slow-spreading Gulf of Mexico. However, because of the fast spreading rate the ridge is expressed as a topographic high and is clearly observed in bathymetry data, allowing mapping of the overall geometry of the ridge reorganization.

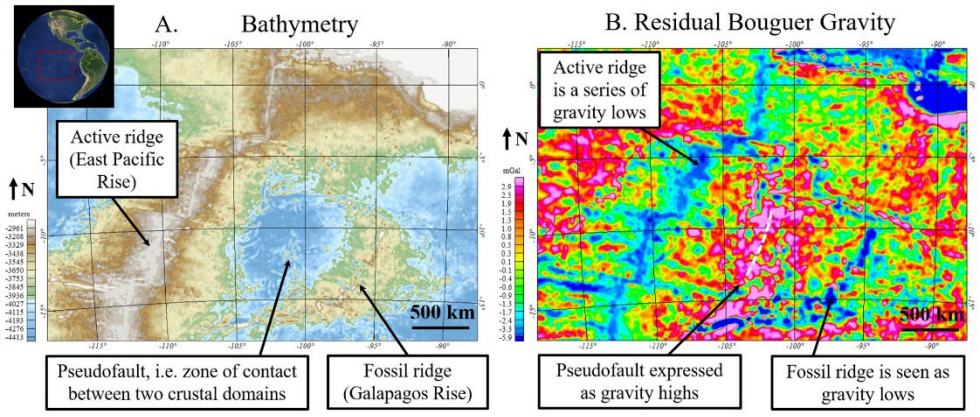

Figure 7. (A) Bathymetry over the East Pacific Rise (EPR, younger, ongoing spreading center) and the Galapagos Rise (extinct fossil spreading center) clearly illustrating the geometry of the ridge reorganization. (B) Residual Bouguer gravity over the same region, suggesting that both fossil and younger ridge segments are associated with pronounced gravity lows that can be used to map them.

Spreading centers in the eastern GOM are not observed in bathymetry, as they are covered with at least 8 km of sediments in the oceanic domain. As we utilized gravity data to map those in eastern GOM (Fig. 4), we analyzed the gravity data from Sandwell et al. (2014) over the EPR as well. We have applied similar corrections sequence to the gravity data over the EPR with one extra step—we performed additional upward continuation of the residual gravity field to an elevation of 8 km. This was done to generate a similar distortion in the gravity signal due to basement being deeper in the GOM than in the EPR (Fig. 7B); both the fossil and the younger active ridge are clearly observed in the gravity data as pronounced gravity lows. This test supports the validity of our interpretation of the overall geometries of the propagated ridge in the eastern GOM from gravity data.

Ridge reorganization during the opening of the eastern GOM explains several geological and geophysical observations. First, it explains the dramatic degree of observed asymmetry in the basin. As already mentioned, the single ridge hypothesis (Fig. 1) leads

to the spreading rate to the north of the ridge to be more than twice as fast as to the south. Although some degree of asymmetry may be expected for the ultra-slow spreading systems and detachment-faults, large-scale asymmetry is usually due to crustal transfer during a ridge reorganization (Müller et al., 2008). Ridge reorganization also explains the striking difference in structure of oceanic crust between two refraction profiles in the study area (Fig. 2A, C). Profile GUMBO4 shows thinner and more uniform crust than the line GUMBO3. We explain the two distinct crustal zones in the oceanic domain of the eastern GOM with spreading variations in the two stages of the basin opening. Last of all, ridge reorganization also explains the observed deep seismicity in the GOM that did not correlate to any previously interpreted geological structure (Fig. 1). The mapped boundary between two distinct oceanic crusts (a thin one associated with a fossil ridge and a thick crust associated with a young ridge), referred as pseudofault (Figs. 4 and 6), corresponds to a gravity high signature in filtered residual Bouguer gravity (similarly to the one over the EPR, Fig. 7). In the GOM, this boundary also agrees with locations of two recorded "lithospheric" earthquakes (i.e., their focal depth was either in crust or in the upper mantle; Figs. 1 and 4). Our study suggests that pseudofault represents a zone of weakness between the two distinct crustal domains produced by two different spreading episodes. This zone appears to be reactivated under current compressional stress (identified from two identical focal mechanisms; Fig. 1). Therefore, the location and a strike of the pseudofault is confirmed with the observed seismicity in the study area.

4. Conclusions

This study concludes that the oceanic crust in the GOM formed in two stages based on the integration of gravity, magnetic, and seismic data. The first spreading episode started presumably at 160 Ma and resulted in approximately 100 km of spreading and generation of thin (~5 km) oceanic crust with a uniform fast seismic velocity profile (Vp ~7 km/s), imaged by GUMBO4 line. This crust is affiliated with the newly identified E-W spreading ridge. Based on our analysis, the estimated spreading rate for this Late Jurassic spreading event was 0.9 cm/yr. A ridge reorganization occurred at 150 Ma, resulting in a NW-SE–oriented spreading center that has been identified by other authors. The crust generated during that second Early Cretaceous spreading episode was imaged by GUMBO3 profile as much thicker (up to 9 km) and with a typical two-layer structure (basaltic layer overlays gabbroic one). Despite the apparent increase in the supply of magmatic material for the second spreading event, the estimated full spreading rate of 1.1 cm/yr is only slightly higher than the initial one. This slow spreading rate is consistent with the overall morphological expression of the spreading centers as valleys, not ridges as imaged by seismic data. The boundary between the two distinct crustal zones is coincident with two deep earthquakes in eastern GOM that were not associated with any geological structure prior to our study. The two-phase spreading model with ridge reorganization in the eastern GOM explains the observed dramatic asymmetry of the basin and the presence of two distinct crustal zones in the oceanic domain as well as observed crustal seismicity that was previously viewed as "intraplate" in origin and presents a novel way to reconstruct the eastern Gulf of Mexico.

Authors' contribution – Irina Filina: supervision, conceptualization, methodology, writing—original draft; Mei Liu: data curation, formal analysis, writing—review and editing; Erin Beutel: conceptualization, validation, writing—review and editing.

Declaration of competing interest – The authors declare that they have no known competing financial interests or personal relationships that could have appeared to influence the work reported in this paper.

Acknowledgments – The authors are very grateful to the editor and three anonymous reviewers for the reviews and constructive criticism. We acknowledge the academic license from Geosoft that was used for spatial analysis.

References

Bird, D., Burke, K., Hall, S., Casey, J., 2005. Gulf of Mexico tectonic history: hotspot tracks, crustal boundaries, and early salt distribution. AAPG Bull. 89 (3), 311–328.

Bown, J.W., White, R.S., 1994. Variation with spreading rate of oceanic crustal thickness and geochemistry. Earth Planet. Sci. Lett. 121, 435–449.

Chen, Y., 1992. Oceanic crustal thickness versus spreading rate. Geophys. Res. Lett. 19, 743–756.

Christeson, G.L., Van Avendonk, H.J.A., Norton, I.O., Snedden, J.W., Eddy, D.R., Karner, G.G., Johnson, C.A., 2014. Deep crustal structure in the eastern Gulf of Mexico. J. Geophys. Res. Solid Earth 119, 6782–6801.

Deighton, I.C., Winter, F., Chisari, D., 2017. Recent high resolution seismic, magnetic and gravity data throws new light on the early development of the Gulf of Mexico. In: AAPG 2017 Annual Convention and Exhibition, Houston, Texas, USA, Search and Discovery, Article #30509.

Eddy, D., Van Avendonk, H., Christeson, G., Norton, I., Karner, G., Johnson, C., Snedden, J., 2014. Deep crustal structure of the northeastern Gulf of Mexico: implications for rift evolution and seafloor spreading. J. Geophys. Res. Solid Earth 119 (9), 6802–6822. https://doi.org/10.1002/2014JB011311.

Filina, et al., 2019. Integrated imaging: a powerful but undervalued tool. The Leading Edge. https://doi.org/10.1190/tle38090720.1.

Galloway, W., 2009. Gulf of Mexico, GEO ExPro, 2009. v. 6, n. 3.

Hudec, M.R., Jackson, M.P.A., Peel, F.J., 2013. Influence of deep Louann structure on the evolution of the northern Gulf of Mexico. AAPG Bull. 97 (10), 1711–1735.

Jian, H., Chen, Y.J., Singh, S.C., Li, J., Zhao, M., Ruan, A., Qiu, X., 2017. Seismic structure and magmatic construction of crust at the ultraslow-spreading Southwest Indian Ridge at 50°28′E. Journal of Geophysical Research: Solid Earth 122 (1), 18–42.

Kim, Y.H., Clayton, R.W., Keppie, F., 2011. Evidence of a collision between the Yucatán Block and Mexico in the Miocene. Geophys. J. Int. 187 (2), 989–1000. https://doi.org/10.1111/j.1365-246X.2011.05191.x. 1 November 2011.

Klingelhöfer, K., Géli, L., Matias, L., Steinsland, N., Mohr, J., 2000. Crustal structure of a super-slow spreading centre: a seismic refraction study of Mohns Ridge, 72°N. Geophys. J. Int. 141 (2), 509–526. https://doi.org/10.1046/j.1365-246x.2000.00098.x.

Kneller, E.A., Johnson, C.A., 2011. Plate kinematics of the Gulf of Mexico based on integrated observations from the Central and South Atlantic. In: Gulf Coast Association of Geological Societies Transactions. 61. pp. 283–299.

Liu, M., Filina, I., 2018. Potential fields modelling in the northeastern Gulf of Mexico. In: AAPG Annual Convention, Salt Lake City, Utah, AAPG Datapages/Search and Discovery, Article #90323.

Lubinski, D.J., Twichell, D.C., 1989. Magnetic and Bathymetric Data from R/V FARNELLA Cruises FRNL85-1, 85-2, and 85-3 in the U.S. Gulf of Mexico EEZ: U.S. Geological Survey Open-File Report 89-156. 6 p. http://pubs.er.usgs.gov/publication/ofr89156.

Lundin, E.R., Doré, A.G., 2017. The Gulf of Mexico and Canada Basin: Genetic Siblings on Either Side of North America. GSA Today 27 (1), 4–11.

Meyer, B., Saltus, R., Chulliat, A., 2017. EMAG2: Earth Magnetic Anomaly Grid (2-Arc-Minute Resolution) Version 3. National Centers for Environmental Information, NOAA Model. https://doi.org/10.7289/V5H70CVX.

Müller, R.D., Sdrolias, M., Gaina, C., Roest, W.R., 2008. Age, spreading rates, and spreading asymmetry of the world's ocean crust. Geochem. Geophys. Geosyst. 9 (4).

Nguyen, L.C., Mann, P., 2016. Gravity and magnetic constraints on the Jurassic opening of the oceanic Gulf of Mexico and the location and tectonic history of the Western Main transform fault along the eastern continental margin of Mexico. Interpretation 4 (1), SC23–SC33.

Pindell, J.L., Kennan, K., 2009. Tectonic evolution of the Gulf of Mexico, Caribbean and northern South America in the mantle reference frame. Geol. Soc. Lond. Spec. Publ. 328, 1–55.

Pindell, J., Miranda, C.E., Ceron, A., Hernandez, L., 2016. Aeromagnetic map constrains Jurassic–Early Cretaceous synrift, break up, and rotational seafloor spreading history in the Gulf of Mexico. In: Mesozoic of the Gulf Rim and Beyond: New Progress in Science and Exploration of the Gulf of Mexico Basin. 35th Annual Gulf Coast Section SEPM Foundation Perkins-Rosen Research Conference, GCSSEPM Foundation, Houston, TX, USA, pp. 123–153.

Sandwell, D.T., Muller, R.D., Smith, W., Garcia, E., Francis, R., 2014. New global marine gravity model from CryoSat-2 and Jason-1 reveals buried tectonic structure. Science 346, 65–67.

Saunders, A., Geiger, L., Rodrigues, K., Hargreaves, P., 2016. The delineation of pre-salt license blocks in the deep offshore Campeche-Yucatan Basin. In: AAPG 2016 Annual Convention and Exhibition, Calgary, Alberta, Canada, Search and Discovery, Article #10867.

Sauter, D., Cannat, M., Rouméjon, S., Andreani, M., Birot, D., Bronner, A., Brunelli, D., Carlut, J., Delacour, A., Guyader, V., MacLeod, C.J., 2013. Continuous exhumation of mantle-derived rocks at the Southwest Indian Ridge for 11 million years. Nature Geoscience 6 (4), 314–320.

Seher, T., Singh, S.C., Crawford, W.C., Escartín, J., 2010. Upper crustal velocity structure beneath the central Lucky Strike Segment from seismic refraction measurements. Geochem. Geophys. Geosyst. 11 (5).

Smith, W., Sandwell, D.T., 1997. Global seafloor topography from satellite altimetry and ship depth soundings. Science 277, 1957–1962.

Snedden, J.W., Norton, I.O., Christeson, G.L., Sanford, J.C., 2014. Interaction of Deepwater Deposition and a Mid-Ocean Spreading Center, Eastern Gulf of Mexico Basin, USA.

Telford, W.M., Geldart, L.P., Sheriff, R.E., 1990. Applied Geophysics. Cambridge University Press.

Thébault, E., Finlay, C.C., Beggan, C.D., Alken, P., Aubert, J., Barrois, O., Bertrand, F., Bondar, T., Boness, A., Brocco, L., Canet, E., 2015. International geomagnetic reference field: the 12th generation. Earth Planets Space 67 (1), 79.

White, R.S., McKenzie, D., O'Nions, R.K., 1992. Ocean crustal thickness from seismic measurements and rare earth element inversions. J. Geophys. Res. 97 (B13), 19683–19715.

White, R.S., Minshull, T.A., Bickle, M.J., Robinson, C.J., 2001. Melt generation at very slow-spreading oceanic ridges: constraints from geochemical and geophysical data. J. Petrol. 42 (6), 1171–1196. https://doi.org/10.1093/petrology/42.6.1171.